

# The double charm decays of $B_c$ Meson in the Perturbative QCD Approach

Zhou Rui <sup>1,2</sup>, Zou Zhitian <sup>1</sup>, and Cai-Dian Lü<sup>1\*</sup>

<sup>1</sup> *Institute of High Energy Physics and Theoretical Physics Center for Science Facilities, Chinese Academy of Sciences, Beijing 100049, People's Republic of China and*

<sup>2</sup> *School of Science, Hebei United University, Tangshan, Hebei 063009, People's Republic of China*

(Dated: February 25, 2013)

## Abstract

We study the double charm decays of  $B_c$  meson, by employing the perturbative QCD approach based on  $k_T$  factorization. In this approach, we include the non-factorizable emission diagrams and W annihilation diagrams, which are neglected in the previous naive factorization approach. The former are important in the color-suppressed modes; while the latter are important in most  $B_c$  decay channels due to the large Cabibbo-Kobayashi-Maskawa matrix elements. We make comparison with those previous naive factorization results for the branching ratios and also give out the theoretical errors that previously missed. We predict the transverse polarization fractions of  $B_c \rightarrow D_{(s)}^{*+} \bar{D}^{*0}, D_{(s)}^{*+} D^{*0}$  decays for the first time. A large transverse polarization contribution that can reach 50%  $\sim$  60% is predicted in some of the  $B_c$  meson decays.

PACS numbers: 13.25.Hw, 12.38.Bx, 14.40.Nd

---

\*Electronic address: lucd@ihep.ac.cn

## I. INTRODUCTION

Since the  $B_c$  meson is the lowest bound state of two different heavy quarks with open flavor, it is stable against strong and electromagnetic annihilation processes. The  $B_c$  meson therefore decays weakly. Furthermore, the  $B_c$  meson has a sufficiently large mass, thus each of the two heavy quarks can decay individually. It has rich decay channels, and provides a very good place to study nonleptonic weak decays of heavy mesons, to test the standard model and to search for any new physics signals [1]. The current running LHC collider will produce much more  $B_c$  mesons than ever before to make this study a bright future.

Within the standard model (SM), for the double charm decays of  $B_{u,d,s}$  mesons, there are penguin operator contributions as well as tree operator contributions. Thus the direct CP asymmetry may be present. However, the double charm decays of  $B_c$  meson are pure tree decay modes, which are particularly well suited to extract the Cabibbo-Kobayashi-Maskawa (CKM) angles due to the absented interference from penguin contributions. As was pointed out in ref. [2] and further elaborated in ref. [3–6], the decays  $B_c \rightarrow D_s^+ D^0, D_s^+ \bar{D}^0$  are the gold-plated modes for the extraction of CKM angle  $\gamma$  through amplitude relations because their decay widths are expected to be at the same order of magnitude. But this needs to be examined by faithful calculations.

Although many investigations on the decays of  $B_c$  to double-charm states have been carried out [4, 5, 7–12] in the literature, there are uncontrolled large theoretical errors with quite different numerical results. In fact, all of these old calculations are based on naive factorization hypothesis, with various form factor inputs. Most of them even did not give any theoretical error estimates because of the non-reliability of these models. Recently, the theory of non-leptonic B decays has been improved quite significantly. Factorization has been proved in many of these decays, thus allow us to give reliable calculations of the hadronic B decays. It is also shown that the non-factorizable contributions and annihilation type contributions, which are neglected in the naive factorization approach, are very important in these decays [13].

The perturbative QCD approach (pQCD) [14] is one of the recently developed theoretical tools based on QCD to deal with the non-leptonic B decays. Utilizing the  $k_T$  factorization instead of collinear factorization, this approach is free of end-point singular-

ity. Thus the Feynman diagrams including factorizable, non-factorizable and annihilation type, are all calculable. Phenomenologically, the pQCD approach successfully predict the charmless two-body B decays [15, 16]. For the decays with a single heavy  $D$  meson in the final states (the momentum of the  $D$  meson is  $\frac{1}{2}m_B(1 - r^2)$ , with  $r = m_D/m_B$ ), it is also proved factorization in the soft-collinear effective theory [17]. Phenomenologically the pQCD approach is also demonstrated to be applicable in the leading order of the  $m_D/m_B$  expansion [18, 19] for this kind of decays. For the double charm decays of  $B_c$  meson, the momentum of the final state  $D$  meson is  $\frac{1}{2}m_{B_c}(1 - 2r^2)$ , which is only slightly smaller than that of the decays with a single D meson final state. The prove of factorization here is thus trivial. The pQCD approach is applicable to this kind of decays. In fact, the double charm decays of  $B_{u,d,s}$  meson have been studied in the pQCD approach successfully [20, 21], with best agreement with experiments. In this paper, we will extend our study to these  $B_c$  decays in the pQCD approach, in order to give predictions on branching ratios and polarization fractions for the experiments to test. Since this study is based on QCD and perturbative expansion, the theoretical error will be controllable than any of the model calculations.

Our paper is organized as follows: We review the pQCD factorization approach and then perform the perturbative calculations for these considered decay channels in Sec.II. The numerical results and discussions on the observables are given in Sec.III. The final section is devoted to our conclusions. Some details of related functions and the decay amplitudes are given in the Appendix.

## II. FRAMEWORK

For the double charm decays of  $B_c$ , only the tree operators of the standard effective weak Hamiltonian contribute. We can divide them into two groups: CKM favored decays with both emission and annihilation contributions and pure emission type decays, which are CKM suppressed. For the former modes, the Hamiltonian is given by:

$$\begin{aligned}\mathcal{H}_{eff} &= \frac{G_F}{\sqrt{2}}V_{cb}^*V_{uq}[C_1(\mu)O_1(\mu) + C_2(\mu)O_2(\mu)], \\ O_1 &= \bar{b}_\alpha\gamma^\mu(1 - \gamma_5)c_\beta \otimes \bar{u}_\beta\gamma_\mu(1 - \gamma_5)q_\alpha, \\ O_2 &= \bar{b}_\alpha\gamma^\mu(1 - \gamma_5)c_\alpha \otimes \bar{u}_\beta\gamma_\mu(1 - \gamma_5)q_\beta,\end{aligned}\tag{1}$$

while the effective Hamiltonian of the latter modes reads

$$\begin{aligned}\mathcal{H}_{eff} &= \frac{G_F}{\sqrt{2}} V_{ub}^* V_{cq} [C_1(\mu) O'_1(\mu) + C_2(\mu) O'_2(\mu)], \\ O'_1 &= \bar{b}_\alpha \gamma^\mu (1 - \gamma_5) u_\beta \otimes \bar{c}_\beta \gamma_\mu (1 - \gamma_5) q_\alpha, \\ O'_2 &= \bar{b}_\alpha \gamma^\mu (1 - \gamma_5) u_\alpha \otimes \bar{c}_\beta \gamma_\mu (1 - \gamma_5) q_\beta,\end{aligned}\tag{2}$$

where  $V(q = d, s)$  are the corresponding CKM matrix elements.  $\alpha, \beta$  are the color indices.  $C_{1,2}$  are Wilson coefficients at renormalization scale  $\mu$ .  $O_{1,2}$  and  $O'_{1,2}$  are the effective four-quark operators.

The factorization theorem allows us to factorize the decay amplitude into the convolution of the hard subamplitude, the Wilson coefficient and the meson wave functions, all of which are well-defined and gauge invariant. It is expressed as

$$C(t) \otimes H(x, t) \otimes \Phi(x) \otimes \exp[-s(P, b) - 2 \int_{1/b}^t \frac{d\mu}{\mu} \gamma_q(\alpha_s(\mu))],\tag{3}$$

where  $C(t)$  are the corresponding Wilson coefficients of effective operators defined in eq.(1,2). Since the transverse momentum of quark is kept in the pQCD approach, the large double logarithm  $\ln^2(Pb)$  (with  $P$  denoting the longitudinal momentum, and  $b$  the conjugate variable of the transverse momentum) to spoil the perturbative expansion. A resummation is thus needed to give a Sudakov factor  $\exp[-s(P, b)]$  [22]. The term after Sudakov is from renormalization group running with  $\gamma_q = -\alpha_s/\pi$  the quark anomalous dimension in axial gauge and  $t$  the factorization scale. All non-perturbative components are organized in the form of hadron wave functions  $\Phi(x)$  (with  $x$  the longitudinal momentum fraction of valence quark inside the meson), which can be extracted from experimental data or other non-perturbative methods. Since the universal non-perturbative dynamics has been factored out, one can evaluate all possible Feynman diagrams for the hard subamplitude  $H(x, t)$  straightforwardly, which include both traditional factorizable and so-called “non-factorizable” contributions. Factorizable and non-factorizable annihilation type diagrams are also calculable without end-point singularity.

### A. Channels with both emission and annihilation contributions

At leading order, there are eight kinds of Feynman diagrams contributing to this type of CKM favored decays according to eq.(1). Here, we take the decay  $B_c \rightarrow D^+ \bar{D}^0$  as

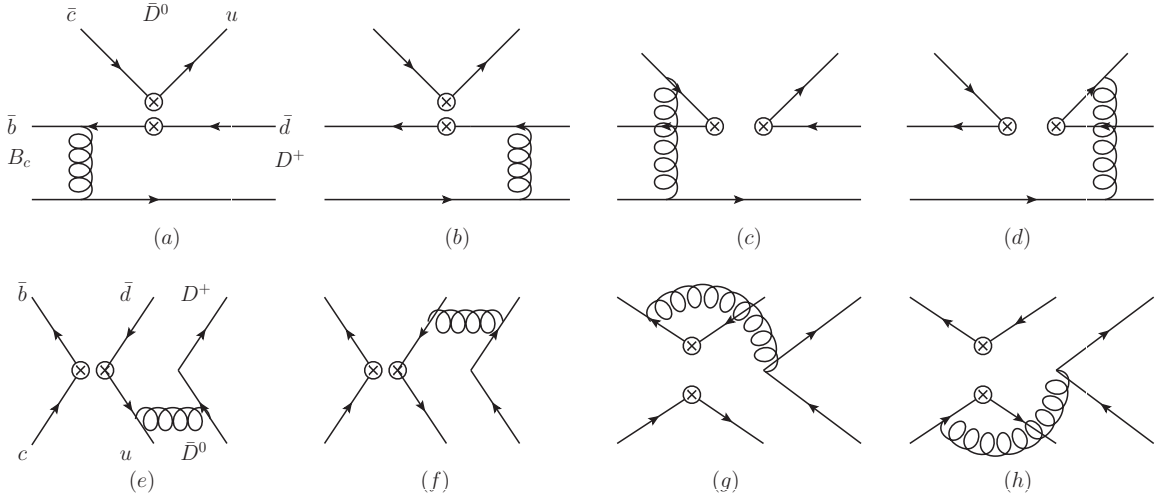


FIG. 1: Feynman diagrams for  $B_c \rightarrow D^+ \bar{D}^0$  decays.

an example, whose Feynman diagrams are shown in Fig.1. The first line are the emission type diagrams, with the first two contributing to the usual form factor; the last two so-called “non-factorizable” diagrams. In fact, the first two diagrams are the only contributions calculated in the naive factorization approach. The second line are the annihilation type diagrams, with the first two factorizable; the last two non-factorizable. The decay amplitude of factorizable diagrams (a) and (b) in Fig.1 is

$$\begin{aligned}
\mathcal{F}_e = & -2\sqrt{\frac{2}{3}}C_F f_B f_3 \pi M_B^4 \int_0^1 dx_2 \int_0^\infty b_1 b_2 db_1 db_2 \phi_2(x_2) \exp\left(-\frac{b_1^2 \omega_B^2}{2}\right) \times \\
& \{[-(r_2 - 2)r_b + 2r_2 x_2 - x_2] \alpha_s(t_a) h_e(\alpha_e, \beta_a, b_1, b_2) S_t(x_2) \exp[-S_{ab}(t_a)] \\
& + 2r_2 \alpha_s(t_b) h_e(\alpha_e, \beta_b, b_2, b_1) S_t(x_1) \exp[-S_{ab}(t_b)]\}, \tag{4}
\end{aligned}$$

where  $r_b = m_b/M_B$ ,  $r_i = m_i/M_B$  ( $i = 2, 3$ ) with  $m_2, m_3$  are the masses of the recoiling charmed meson and the emitting charmed meson, respectively;  $C_F = 4/3$  is a color factor;  $f_3$  is the decay constant of the charmed meson, which emitted from the weak vertex. The factorization scales  $t_{a,b}$  are chosen as the maximal virtuality of internal particles in the hard amplitude, in order to suppress the higher order corrections [23]. The function  $h_e$  and the Sudakov factor  $\exp[-S]$  are displayed in the Appendix B.  $D$  meson distribution amplitude  $\phi(x)$  are given in Appendix C. The factor  $S_t(x)$  is the jet function resulting from the threshold resummation, whose definitions can be found in [24].

The formula for non-factorizable emission diagrams Fig. 1 (c) and (d) contain the

kinematics variables of all the three mesons. Its expression is:

$$\begin{aligned}\mathcal{M}_e = & -\frac{8}{3}C_F f_B \pi M_B^4 \int_0^1 dx_2 dx_3 \int_0^\infty b_2 b_3 db_2 db_3 \phi_2(x_2) \phi_3(x_3) \exp(-\frac{b_2^2 \omega_B^2}{2}) \times \\ & \{[1 - x_1 - x_3 - r_2(1 - x_2)]\alpha_s(t_c)h_e(\beta_c, \alpha_e, b_3, b_2) \exp[-S_{cd}(t_c)] - \\ & [1 - x_1 - x_2 + x_3 - r_2(1 - x_2)]\alpha_s(t_d)h_e(\beta_d, \alpha_e, b_3, b_2) \exp[-S_{cd}(t_d)]\}. \quad (5)\end{aligned}$$

Generally, for charmless decays of B meson, the non-factorizable contributions of the emission diagrams are small due to the cancelation between Fig. 1 (c) and (d). While for double charm decays with the light meson replaced by a charmed meson, since the heavy  $\bar{c}$  quark and the light quark is not symmetric, the non-factorizable emission diagrams ought to give remarkable contributions. This has been shown in the pQCD calculation of  $B \rightarrow D\pi$  decays for a very large branching ratios of color-suppressed modes [25] and proved by the B factory experiments.

The decay amplitude of factorizable annihilation diagrams Fig. 1 (e) and (f) involve only the two final states charmed meson wave functions, shown as

$$\begin{aligned}\mathcal{F}_a = & -8C_F f_B \pi M_B^4 \int_0^1 dx_2 dx_3 \int_0^\infty b_2 b_3 db_2 db_3 \phi_2(x_2) \phi_3(x_3) \times \\ & \{[1 - x_2]\alpha_s(t_e)h_e(\alpha_a, \beta_e, b_2, b_3) \exp[-S_{ef}(t_e)]S_t(x_3) - \\ & [1 - x_3]\alpha_s(t_f)h_e(\alpha_a, \beta_f, b_3, b_2) \exp[-S_{ef}(t_f)]S_t(x_2)\}. \quad (6)\end{aligned}$$

For the non-factorizable annihilation diagrams Fig. 1 (g) and (h), the decay amplitude is

$$\begin{aligned}\mathcal{M}_a = & \frac{8}{3}C_F f_B \pi M_B^4 \int_0^1 dx_2 dx_3 \int_0^\infty b_1 b_2 db_1 db_2 \phi_2(x_2) \phi_3(x_3) \exp(-\frac{b_1^2 \omega_B^2}{2}) \\ & \times \{[x_1 + x_3 - 1 - r_c]\alpha_s(t_g)h_e(\beta_g, \alpha_a, b_1, b_2) \exp[-S_{gh}(t_g)] \\ & - [r_b - x_2]\alpha_s(t_h)h_e(\beta_h, \alpha_a, b_1, b_2) \exp[-S_{gh}(t_h)]\}, \quad (7)\end{aligned}$$

where  $r_c = m_c/M_B$ , with  $m_c$  the mass of c quark in  $B_c$  meson. Finally, the total decay amplitude for  $B_c \rightarrow D^+ \bar{D}^0$  can be given by

$$\mathcal{A}(B_c \rightarrow D^+ \bar{D}^0) = V_{cb}^* V_{ud} [a_2 \mathcal{F}_e + C_2 \mathcal{M}_e + a_1 \mathcal{F}_a + C_1 \mathcal{M}_a], \quad (8)$$

with the combinations of Wilson coefficients  $a_1 = C_2 + C_1/3$  and  $a_2 = C_1 + C_2/3$ , characterizing the color favored contribution and the color-suppressed contribution in the naive factorization, respectively. The total decay amplitudes of  $B_c \rightarrow D_s^+ \bar{D}^0$ ,  $B_c \rightarrow D^+ \bar{D}^{*0}$  and

$B_c \rightarrow D_s^+ \bar{D}^{*0}$  can be obtained from eq.(8) with the following replacement:

$$\begin{aligned}\mathcal{A}(B_c \rightarrow D_s^+ \bar{D}^0) &= V_{cb}^* V_{us} [a_2 \mathcal{F}_e + C_2 \mathcal{M}_e + a_1 \mathcal{F}_a + C_1 \mathcal{M}_a]|_{D^+ \rightarrow D_s^+}, \\ \mathcal{A}(B_c \rightarrow D^+ \bar{D}^{*0}) &= V_{cb}^* V_{ud} [a_2 \mathcal{F}_e + C_2 \mathcal{M}_e + a_1 \mathcal{F}_a + C_1 \mathcal{M}_a]|_{\bar{D}^0 \rightarrow \bar{D}^{*0}}, \\ \mathcal{A}(B_c \rightarrow D_s^+ \bar{D}^{*0}) &= V_{cb}^* V_{us} [a_2 \mathcal{F}_e + C_2 \mathcal{M}_e + a_1 \mathcal{F}_a + C_1 \mathcal{M}_a]|_{D^+ \rightarrow D_s^+, \bar{D}^0 \rightarrow \bar{D}^{*0}}.\end{aligned}\quad (9)$$

Comparing our eq.(8,9) with the formulas of previous naive factorization approach [4, 5, 7–10], it is easy to see that only the first term appearing in eq.(8,9) are calculated in the previous naive factorization approach. The second, third and fourth terms in these equations, are the corresponding non-factorizable emission type contribution, factorizable and non-factorizable annihilation type contributions, respectively, which are all new calculations.

In  $B_c \rightarrow D_{(s)}^{*+} \bar{D}^{*0}$  decays, the two vector mesons in the final states have the same helicity due to angular momentum conservation, therefore only three different polarization states, one longitudinal and two transverse for both vector mesons, are possible. The decay amplitude can be decomposed as

$$\mathcal{A} = \mathcal{A}^L + \mathcal{A}^N \epsilon_2^T \cdot \epsilon_3^T + i \mathcal{A}^T \epsilon_{\alpha\beta\rho\sigma} n^\alpha v^\beta \epsilon_2^{T\rho} \epsilon_3^{T\sigma}, \quad (10)$$

where  $\epsilon_2^T, \epsilon_3^T$  are the transverse polarization vectors for the two vector charmed mesons, respectively.  $\mathcal{A}^L$  corresponds to the contributions of longitudinal polarization;  $\mathcal{A}^N$  and  $\mathcal{A}^T$  corresponds to the contributions of normal and transverse polarization, respectively. And the total amplitudes  $\mathcal{A}^{L,N,T}$  have the same structures as eq.(8,9). The factorization formulae for the longitudinal, normal and transverse polarizations are listed in Appendix A.

For  $B_c \rightarrow D_{(s)}^{*+} \bar{D}^0$  decays, only the longitudinal polarization of  $D_{(s)}^{*+}$  meson will contribute, due to the angular momentum conservation. We can obtain their decay amplitudes from the longitudinal polarization amplitudes for the  $B_c \rightarrow D_{(s)}^{*+} \bar{D}^{*0}$  decays with the replacement  $\bar{D}^{*0} \rightarrow \bar{D}^0$ .

## B. Channels with pure emission type decays

There are also eight kinds of Feynman diagrams contributing to  $B_c \rightarrow D_{(s)}^{(*)+} D^{(*)0}$  decays according to eq.(2), but all are emission type. Taking the decay  $B_c \rightarrow D^+ D^0$  as

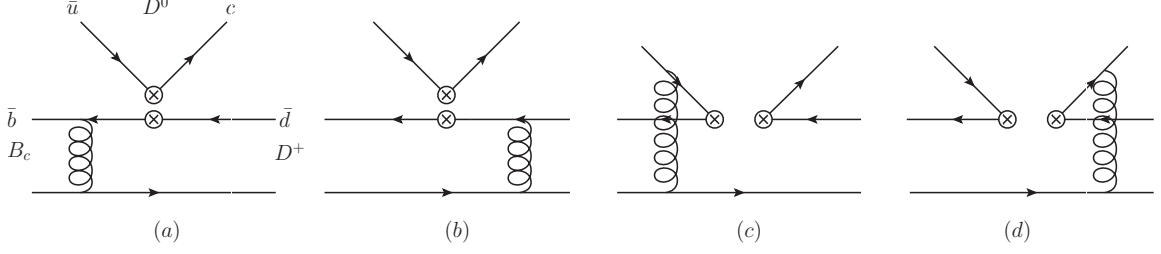


FIG. 2: Color-suppressed emission diagrams contributing to the  $B_c \rightarrow D^+ D^0$  decays.

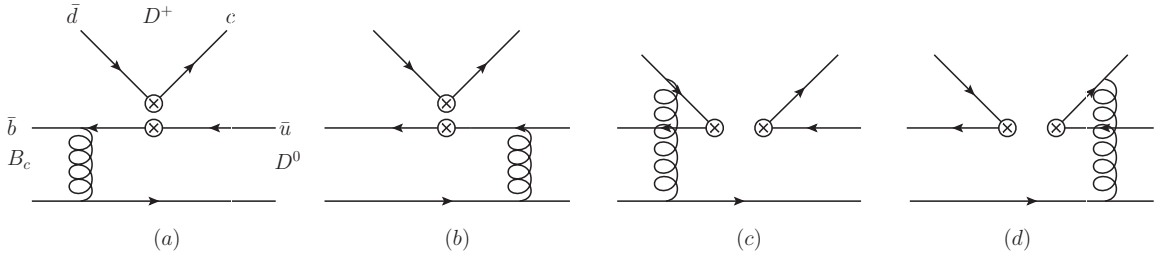


FIG. 3: Color-favored emission diagrams contributing to the  $B_c \rightarrow D^+ D^0$  decays.

an example, Fig. 2 are the color-suppressed emission diagrams while Fig. 3 are the color-favored emission diagrams. We mark the subscript 2 and 3 to denote the contributions from Fig. 2 and Fig. 3, respectively. The decay amplitude of factorization emission diagrams  $\mathcal{F}_{e2}$ , coming from Fig. 2 (a,b), is similar to eq.(4), but with the replacement  $\bar{D}^0 \rightarrow D^0$ . While the decay amplitude of non-factorization emission diagram  $\mathcal{M}_{e2}$ , coming from Fig. 2 (c,d), is different from eq.(5), since the heavy c quark and the light anti-quark are not symmetric. The expression of the non-factorizable emission diagram is

$$\begin{aligned} \mathcal{M}_{e2} = & -\frac{8}{3}C_F f_B \pi M_B^4 \int_0^1 dx_2 dx_3 \int_0^\infty b_2 b_3 db_2 db_3 \phi_2(x_2) \phi_3(x_3) \exp\left(-\frac{b_2^2 \omega_B^2}{2}\right) \\ & \times \{[2 - x_1 - x_2 - x_3 - r_2(1 - x_2)]\alpha_s(t_c) h_e(\beta_c, \alpha_e, b_3, b_2) \exp[-S_{cd}(t_c)] - \\ & [x_3 - x_1 - r_2(1 - x_2)]\alpha_s(t_d) h_e(\beta_d, \alpha_e, b_3, b_2) \exp[-S_{cd}(t_d)]\}. \end{aligned} \quad (11)$$

By exchanging the two final states charmed mesons in Fig. 2, one can obtain the corresponding decay amplitudes formulae  $\mathcal{F}_{e3}$  and  $\mathcal{M}_{e3}$  for Fig. 3. The total decay amplitude of  $B_c \rightarrow D^+ D^0$  decay can be written as

$$\mathcal{A}(B_c \rightarrow D^+ D^0) = V_{ub}^* V_{cd} [a_2 \mathcal{F}_{e2} + C_2 \mathcal{M}_{e2} + a_1 \mathcal{F}_{e3} + C_1 \mathcal{M}_{e3}]. \quad (12)$$



If the final recoiling meson is the vector  $D^*$  meson, the decay amplitudes of factorization emission diagrams and non-factorization emission diagrams are given as

$$\begin{aligned}\mathcal{F}_{e2}^* &= -2\sqrt{\frac{2}{3}}C_F f_B f_3 \pi M_B^4 \int_0^1 dx_2 \int_0^\infty b_1 b_2 db_1 db_2 \phi_2(x_2) \exp(-\frac{b_1^2 \omega_B^2}{2}) \\ &\quad \times \{[-(r_2 - 2)r_b + 2r_2 x_2 - x_2] \alpha_s(t_a) h_e(\alpha_e, \beta_a, b_1, b_2) S_t(x_2) \exp[-S_{ab}(t_a)] \\ &\quad + r_2^2 \alpha_s(t_b) h_e(\alpha_e, \beta_b, b_2, b_1) S_t(x_1) \exp[-S_{ab}(t_b)]\},\end{aligned}\quad (13)$$

$$\begin{aligned}\mathcal{M}_{e2}^* &= -\frac{8}{3}C_F f_B \pi M_B^4 \int_0^1 dx_2 dx_3 \int_0^\infty b_2 b_3 db_2 db_3 \phi_2(x_2) \phi_3(x_3) \exp(-\frac{b_2^2 \omega_B^2}{2}) \\ &\quad \times \{[2 - x_1 - x_2 - x_3 - r_2(1 - x_2)] \alpha_s(t_c) h_e(\beta_c, \alpha_e, b_3, b_2) \exp[-S_{cd}(t_c)] - \\ &\quad [x_3 - x_1 + r_2(1 - x_2)] \alpha_s(t_d) h_e(\beta_d, \alpha_e, b_3, b_2) \exp[-S_{cd}(t_d)]\}.\end{aligned}\quad (14)$$

The total decay amplitudes for other pure emission type decays are then

$$\begin{aligned}\mathcal{A}(B_c \rightarrow D_s^+ D^0) &= V_{ub}^* V_{cs} [a_2 \mathcal{F}_{e2} + C_2 \mathcal{M}_{e2} + a_1 \mathcal{F}_{e3} + C_1 \mathcal{M}_{e3}], \\ \mathcal{A}(B_c \rightarrow D^+ D^{*0}) &= V_{ub}^* V_{cd} [a_2 \mathcal{F}_{e2} + C_2 \mathcal{M}_{e2} + a_1 \mathcal{F}_{e3}^* + C_1 \mathcal{M}_{e3}^*], \\ \mathcal{A}(B_c \rightarrow D^{*+} D^0) &= V_{ub}^* V_{cd} [a_2 \mathcal{F}_{e2}^* + C_2 \mathcal{M}_{e2}^* + a_1 \mathcal{F}_{e3} + C_1 \mathcal{M}_{e3}], \\ \mathcal{A}(B_c \rightarrow D_s^+ D^{*0}) &= V_{ub}^* V_{cs} [a_2 \mathcal{F}_{e2} + C_2 \mathcal{M}_{e2} + a_1 \mathcal{F}_{e3}^* + C_1 \mathcal{M}_{e3}^*], \\ \mathcal{A}(B_c \rightarrow D_s^{*+} D^0) &= V_{ub}^* V_{cs} [a_2 \mathcal{F}_{e2}^* + C_2 \mathcal{M}_{e2}^* + a_1 \mathcal{F}_{e3} + C_1 \mathcal{M}_{e3}].\end{aligned}\quad (15)$$

The  $B_c \rightarrow D_{(s)}^{*+} D^{*0}$  decays have a similar situation to  $B_c \rightarrow D_{(s)}^{*+} \bar{D}^{*0}$ , their factorization formulae are also listed in Appendix.A.

### III. NUMERICAL RESULTS

In this section, we summarize the numerical results and analysis in the double charm decays of the  $B_c$  meson. Some input parameters needed in the pQCD calculation are listed in Table I.

#### A. The Form Factors

The diagrams (a) and (b) in Fig.1 or Fig.3 give the contribution for  $B_c \rightarrow D_{(s)}^{(*)}$  transition form factor at  $q^2 = 0$  point. Our predictions of the form factors are collected in

TABLE I: Parameters we used in numerical calculation [26]

Mass(GeV)	$M_W = 80.399$	$M_{B_c} = 6.277$	$m_b = 4.2$	$m_c = 1.27$
CKM	$ V_{ub}  = (3.47^{+0.16}_{-0.12}) \times 10^{-3}$	$ V_{ud}  = 0.97428^{+0.00015}_{-0.00015}$	$ V_{us}  = 0.2253^{+0.0007}_{-0.0007}$	
	$ V_{cs}  = 0.97345^{+0.00015}_{-0.00016}$	$ V_{cd}  = 0.2252^{+0.0007}_{-0.0007}$	$ V_{cb}  = 0.0410^{+0.0011}_{-0.0007}$	
Decay constants(MeV)	$f_{B_c} = 489$	$f_D = 206.7 \pm 8.9$	$f_{D_s} = 257.5 \pm 6.1$	
Lifetime	$\tau_{B_c} = 0.453 \times 10^{-12}\text{s}$			

 TABLE II: The form factors for  $B_c \rightarrow D_{(s)}^{(*)}$  at  $q^2 = 0$  evaluated in the pQCD approach. The uncertainties are from the hadronic parameters. For comparison, we also cite the theoretical estimates of other models.

	This work	Kiselev [4] <sup>a</sup>	IKP [5]	WSL [27]	DSV [28]	DW [29] <sup>b</sup>
$F^{B_c \rightarrow D}$	$0.14^{+0.01}_{-0.02}$	0.32 [0.29]	0.189	0.16	0.075	0.255
$F^{B_c \rightarrow D_s}$	$0.19^{+0.02}_{-0.01}$	0.45 [0.43]	0.194	0.28	0.15	—
$A_0^{B_c \rightarrow D^*}$	$0.12^{+0.02}_{-0.01}$	0.35 [0.37]	0.133	0.09	0.081	0.257
$A_0^{B_c \rightarrow D_s^*}$	$0.17^{+0.01}_{-0.01}$	0.47 [0.52]	0.142	0.17	0.16	—

<sup>a</sup>The non-bracket (bracketed) results are evaluated in sum rules (potential model)

<sup>b</sup>We quote the result with  $\omega = 0.7\text{GeV}$

Table II. The error is from the combined uncertainty in the hadronic parameters: (1) the shape parameters:  $\omega_B = 0.60 \pm 0.05$  for  $B_c$  meson wave function,  $a_D = (0.5 \pm 0.1)\text{GeV}$  for  $D^{(*)}$  meson and  $a_{D_s} = (0.4 \pm 0.1)\text{GeV}$  for  $D_s^{(*)}$  meson wave function [20]; (2) the decay constants in the wave functions of charmed mesons, which are given in Table I. Since the uncertainties from decay constants of  $D_{(s)}$  and the shape parameters of the wave functions are very small, the relevant uncertainties to the form factors are also very small. We can see that the  $SU(3)$  symmetry breaking effects between  $B_c$  to  $D^{(*)}$  and  $B_c$  to  $D_s^{(*)}$  form factors are large, as the decay constant of  $D_s$  is about one-fifth larger than that of the  $D$  meson.

In the literature there are already lots of studies on  $B_c \rightarrow D_{(s)}^{(*)}$  transition form factors [4, 5, 27–29], whose results are collected in Table II. Our results are generally close to the covariant light-front quark model results of [27] and the constituent quark model results of [5]. However, other results collected in Table II, especially for the QCD sum rules (QCDSR) [4] and the Bauer, Stech and Wirbel (BSW) model [28] deviate a lot

numerically. The predictions of QCDSR [4] are larger than those in other works [5, 27–29]. The reason is that they have taken into account the  $\alpha_s/v$  corrections and the form factors are enhanced by 3 times due to the Coulomb renormalization of the quark-meson vertex for the heavy quarkonium  $B_c$ . The results of BSW model [28] are quite small due to the less overlap of the initial and final states wave functions. Although, the included flavor dependence of the average transverse quark momentum in the mesons can enhance the form factors for  $B_c \rightarrow D_{(s)}^*$  transitions, their predictions are still smaller than other models. The large differences in different models can be discriminated by the future LHC experiments.

## B. Branching Ratios

With the decays amplitudes  $\mathcal{A}$  obtained in Sec.II, the branching ratio  $\mathcal{BR}$  reads as

$$\mathcal{BR} = \frac{G_F \tau_{B_c}}{32\pi M_B} \sqrt{(1 - (r_2 + r_3)^2)(1 - (r_2 - r_3)^2)} |\mathcal{A}|^2. \quad (16)$$

As stated in Sec II, the contributions from the penguin operators are absent, since the penguins add an even number of charmed quarks, while there is already one from the initial state. There should be no CP violation in these processes. We tabulate the branching ratios of the considered decays in Table III and IV. The processes (1)-(4) in Table III have a comparatively large branching ratios ( $10^{-5}$ ) with the CKM factor  $V_{cb}^* V_{ud} \sim \lambda^2$ . While the branching ratios of other processes are relatively small due to the CKM factor suppression. Especially for the processes (1)-(4) in Table IV, these channels are suppressed by CKM element  $V_{ub}/V_{cb}$  and  $V_{cd}/V_{ud}$ . Thus their branching ratios are three order magnitudes smaller.

For comparison, we also cite other theoretical results [4, 5, 7, 8, 10] for the double charm decays of  $B_c$  meson in Tables III and IV. In general, the results of the various model calculations are of the same order of magnitude for most channels. However the difference between different model calculations is quite large. This is expected from the large difference of input parameters, especially the large difference of form factors shown in Table II. As stated in the introduction, all the calculations of these  $B_c$  to two D meson decays in the literature use the same naive factorization approach. Their difference relies only on the input form factors and decay constants. Therefore the comparison of

TABLE III: Branching ratios ( $10^{-6}$ ) of the CKM favored decays with both emission and annihilation contributions, together with results from other models. The errors for these entries correspond to the uncertainties in the input hadronic quantities, from the CKM matrix elements, and the scale dependence, respectively.

	channels	This work	Kiselev[4]	IKP[5]	IKS[7]	LC[8]	CF[10]
1	$B_c \rightarrow D^+ \bar{D}^0$	$32^{+6+1+2}_{-6-1-4}$	53	32	33	86	8.4
2	$B_c \rightarrow D^+ \bar{D}^{*0}$	$34^{+7+2+3}_{-6-1-3}$	75	83	38	75	7.5
3	$B_c \rightarrow D^{*+} \bar{D}^0$	$12^{+3+1+0}_{-3-0-1}$	49	17	9	30	84
4	$B_c \rightarrow D^{*+} \bar{D}^{*0}$	$34^{+9+2+0}_{-8-1-0}$	330	84	21	55	140
5	$B_c \rightarrow D_s^+ \bar{D}^0$	$2.3^{+0.4+0.1+0.2}_{-0.4-0.1-0.2}$	4.8	1.7	2.1	4.6	0.6
6	$B_c \rightarrow D_s^+ \bar{D}^{*0}$	$2.6^{+0.4+0.1+0.1}_{-0.6-0.1-0.2}$	7.1	4.3	2.4	3.9	0.53
7	$B_c \rightarrow D_s^{*+} \bar{D}^0$	$0.7^{+0.1+0.0+0.0}_{-0.2-0.0-0.0}$	4.5	0.95	0.65	1.8	5
8	$B_c \rightarrow D_s^{*+} \bar{D}^{*0}$	$2.8^{+0.7+0.1+0.1}_{-0.6-0.1-0.0}$	26	4.7	1.6	3.5	8.4

TABLE IV: Branching ratios ( $10^{-7}$ ) of the CKM suppressed decays with pure emission contributions, together with results from other models. The errors for these entries correspond to the uncertainties in the input hadronic quantities, from the CKM matrix elements, and the scale dependence, respectively.

	channels	This work	Kiselev[4]	IKP[5]	IKS[7]
1	$B_c \rightarrow D^+ D^0$	$1.0^{+0.2+0.1+0.0}_{-0.1-0.0-0.0}$	3.2	1.1	3.1
2	$B_c \rightarrow D^+ D^{*0}$	$0.7^{+0.1+0.1+0.0}_{-0.2-0.0-0.0}$	2.8	0.25	0.52
3	$B_c \rightarrow D^{*+} D^0$	$0.9^{+0.1+0.1+0.0}_{-0.2-0.0-0.0}$	4.0	3.8	4.4
4	$B_c \rightarrow D^{*+} D^{*0}$	$0.8^{+0.2+0.1+0.2}_{-0.1-0.0-0.0}$	15.9	2.8	2.0
5	$B_c \rightarrow D_s^+ D^0$	$30^{+5+3+1}_{-4-2-1}$	66	25	74
6	$B_c \rightarrow D_s^+ D^{*0}$	$19^{+3+2+0}_{-3-1-1}$	63	6	13
7	$B_c \rightarrow D_s^{*+} D^0$	$25^{+4+2+0}_{-3-2-1}$	85	69	93
8	$B_c \rightarrow D_s^{*+} D^{*0}$	$24^{+3+2+1}_{-3-2-1}$	404	54	45

results with any of them is straightforward. Larger branching ratios come always with the larger form factors. As stated in the previous subsection, our results of form factors are comparable with the relativistic constituent quark model (RCQM) [5, 7], thus our branching ratios in Table III are also comparable with theirs except for the processes  $B_c \rightarrow D^{*+} \bar{D}^{*0}$  and  $B_c \rightarrow D_s^{*+} \bar{D}^{*0}$ . Due to the sizable contributions of transverse polarization amplitudes, our branching ratios are larger than those in RCQM model, whose transverse contribution is negligible.

Since all the previous calculations in the literature are model calculations, it is difficult for them to give the theoretical error estimations. In our pQCD approach, the factorization holds at the leading order expansion of  $m_D/m_B$ . At this order, we can do the systematical calculation, so as to the error estimations in the tables. The first error in these entries is estimated from the hadronic parameters: (1) the shape parameters:  $\omega_B = 0.60 \pm 0.05$  for  $B_c$  meson,  $a_D = (0.5 \pm 0.1)\text{GeV}$  for  $D^{(*)}$  meson and  $a_{D_s} = (0.4 \pm 0.1)\text{GeV}$  for  $D_s^{(*)}$  meson [20]; (2) the decay constants in the wave functions of charmed mesons, which are given in Table I. The second error is from the uncertainty in the CKM matrix elements, which are also given in Table I. The third error arises from the hard scale  $t$  varying from  $0.75t$  to  $1.25t$ , which characterizing the size of next-to-leading order QCD contributions. The not large errors of this type indicate that our perturbative expansion indeed hold. It is easy to see that the most important uncertainty in our approach comes from the hadronic parameters. The total theoretical error is in general around 10% to 30% in size.

The eight CKM favored channels (proportional to  $|V_{cb}|$ ) in Table III receive contributions from both emission diagrams and annihilation diagrams. From Fig.1, one can find that the contributions from the factorizable emission diagrams are color-suppressed. The naive factorization approach can not give reliable predictions due to large non-factorizable contributions [30]. As was pointed out in Sec.II, the non-factorizable emission diagrams give large contributions in pQCD approach because the asymmetry of the two quarks in charmed mesons. Thus, the branching ratios of these decays are dominated by the non-factorizable emission diagrams.

The eight CKM suppressed channels (proportional to  $|V_{ub}|$ ) in Table IV can occur only via emission type diagrams. There are two types of emission diagrams in these decays, one is color-suppressed, one is color favored. It is expected that the color-favored factorizable amplitude  $\mathcal{F}_{e3}$  dominates in eq.(15). However, the non-factorizable contribution  $\mathcal{M}_{e2}$ , proportional to the large  $C_2$ , is enhanced by the Wilson coefficient. Numerically it is indeed comparable to the color-favored factorizable amplitude. This large non-factorizable contribution has already been shown in the similar  $B \rightarrow D\pi$  decays theoretically and experimentally [25]. In all of these channels the non-factorizable contributions play a very important role, therefore the branching ratios predicted in table III and IV are not like the previous naive factorization approach calculations [4, 5, 7, 8, 10]. They are

TABLE V: The transverse polarizations fractions (%) for  $B_c \rightarrow VV$ . The errors correspond to the uncertainties in the hadronic parameters and the scale dependence, respectively.

	$B_c \rightarrow D^{*+} \bar{D}^{*0}$	$B_c \rightarrow D_s^{*+} \bar{D}^{*0}$	$B_c \rightarrow D^{*+} D^{*0}$	$B_c \rightarrow D_s^{*+} D^{*0}$
$\mathcal{R}_T$	$58^{+3+1}_{-3-0}$	$68^{+2+1}_{-2-1}$	$4^{+1+1}_{-1-1}$	$6^{+1+2}_{-0-1}$

not simply proportional to the corresponding form factors any more, but with a very complicated manner, since we have also additional annihilation type contributions.

From Table III and IV, one can see that as it was expected the magnitudes of the branching ratios of the decays  $B_c \rightarrow D_s^+ \bar{D}^0$  and  $B_c \rightarrow D_s^+ D^0$  are very close to each other. In our numerical results, the ratio of the two decay widths is estimated as  $\frac{\Gamma(B_c \rightarrow D_s^+ D^0)}{\Gamma(B_c \rightarrow D_s^+ \bar{D}^0)} \approx 1.3$ . They are very suitable for extracting the CKM angle  $\gamma$  though the amplitude relations. Hopefully they will be measured in the experiments soon. However, the decays  $B_c \rightarrow D^+ \bar{D}^0, D^+ D^0$  are problematic from the methodic point of view for  $\mathcal{BR}(B_c \rightarrow D^+ D^0) \ll \mathcal{BR}(B_c \rightarrow D^+ \bar{D}^0)$ . The corresponding ratio in  $B_c \rightarrow D^+ D^0, D^+ \bar{D}^0$  decays is  $\frac{\Gamma(B_c \rightarrow D^+ D^0)}{\Gamma(B_c \rightarrow D^+ \bar{D}^0)} \sim 10^{-3}$ , which confirm the latter decay modes are not useful to determine the angle  $\gamma$  experimentally.

For the  $B_c$  decays to two vector mesons, the decays amplitudes  $\mathcal{A}$  are defined in the helicity basis

$$\mathcal{A} = \sum_{i=0,+,-} |\mathcal{A}_i|^2, \quad (17)$$

where the helicity amplitudes  $\mathcal{A}_i$  have the following relationships with  $\mathcal{A}^{L,N,T}$

$$\mathcal{A}_0 = \mathcal{A}^L, \quad \mathcal{A}_{\pm} = \mathcal{A}^N \pm \mathcal{A}^T. \quad (18)$$

We also calculate the transverse polarization fractions  $\mathcal{R}_T$  of the  $B_c \rightarrow D_{(s)}^* D^*$  decays, with the definition given by

$$\mathcal{R}_T = \frac{|\mathcal{A}_+|^2 + |\mathcal{A}_-|^2}{|\mathcal{A}_0|^2 + |\mathcal{A}_+|^2 + |\mathcal{A}_-|^2}. \quad (19)$$

This should be the first time theoretical predictions in the literature, which are absent in all the naive factorization calculations. According to the power counting rules in the factorization assumption, the longitudinal polarization should be dominant due to the quark helicity analysis. Our predictions for the transverse polarization fractions of

the decays  $B_c \rightarrow D_{(s)}^{*+} D^{*0}$ , which are given in Table V, are indeed small, since the two transverse amplitudes are down by a power of  $r_2$  or  $r_3$  comparing with the longitudinal amplitudes. However, for  $B_c \rightarrow D_{(s)}^{*+} \bar{D}^{*0}$  decays, the most important contributions for these two decay channels are from the non-factorizable tree diagrams in Fig. 1(c) and 1(d). With an additional gluon, the transverse polarization in the non-factorizable diagrams does not encounter helicity flip suppression. The transverse polarization is at the same order as longitudinal polarization. Therefore, we can expect the transverse polarizations take a larger ratio in the branching ratios, which can reach  $\sim 60\%$ . The fact that the non-factorizable contribution can give large transverse polarization contribution is also observed in the  $B^0 \rightarrow \rho^0 \rho^0, \omega \omega$  decays [31] and in the  $B_c \rightarrow D_s^{*+} \omega$  decay [32].

#### IV. CONCLUSION

All the previous calculations in the literature for the  $B_c$  meson decays to two charmed mesons are based on the very simple naive factorization approach. The branching ratios predicted in this kind of model calculation depend heavily on the input form factors. Since all of these modes contain dominant or large contributions from color-suppressed diagrams, the predicted branching ratios are also not stable due to the large unknown non-factorizable contributions. In this paper, we have performed a systematic analysis of the double charm decays of the  $B_c$  meson in the pQCD approach based on  $k_T$  factorization theorem, which is free of end-point singularities. All topologies of decay amplitudes are calculable in the same framework, including the non-factorizable one and annihilation type. It is found that the non-factorizable emission diagrams give a remarkable contribution. There is no CP violation for all these decays within the standard model, since there are only tree operators contributions. The predicted branching ratios range from very small numbers of  $\mathcal{O}(10^{-8})$  up to the largest branching fraction of  $\mathcal{O}(10^{-5})$ . Since all of the previous naive factorization calculations did not give the theoretical uncertainty in the numerical results, it is not easy to compare our results with theirs. The theoretical uncertainty study in the pQCD approach shows that our numerical results are reliable, which may be tested in the upcoming experimental measurements. We predict the transverse polarization fractions of the  $B_c$  decays with two vector  $D^*$  mesons in the final states for the first time. Due to the cancelation of some hadronic parameters in

the ratio, the polarization fractions are predicted with less theoretical uncertainty. The transverse polarization fractions are large in some channels, which mainly come from the non-factorizable emission diagrams.

### Acknowledgments

We thank Hsiang-nan Li and Fusheng Yu for helpful discussions. This work is partially supported by National Natural Science Foundation of China under the Grant No. 11075168; Natural Science Foundation of Zhejiang Province of China, Grant No. Y606252 and Scientific Research Fund of Zhejiang Provincial Education Department of China, Grant No. 20051357.

### Appendix A: Factorization formulas for $B_c \rightarrow VV$

In the  $B_c$  decays to two vector meson final states, we use the superscript L, N and T to denote the contributions from longitudinal polarization, normal polarization and transverse polarization, respectively. For the CKM favored  $B_c \rightarrow D_{(s)}^{*+} \bar{D}^{*0}$  decays, the decay amplitudes for different polarizations are

$$\begin{aligned} \mathcal{F}_e^L = & -2\sqrt{\frac{2}{3}}C_F f_B f_3 \pi M_B^4 \int_0^1 dx_2 \int_0^\infty b_1 b_2 db_1 db_2 \phi_2(x_2) \exp(-\frac{b_1^2 \omega_B^2}{2}) \times \\ & \{[-(r_2 - 2)r_b + 2r_2 x_2 - x_2] \alpha_s(t_a) h_e(\alpha_e, \beta_a, b_1, b_2) S_t(x_2) \exp[-S_{ab}(t_a)] \\ & + r_2^2 \alpha_s(t_b) h_e(\alpha_e, \beta_b, b_2, b_1) S_t(x_1) \exp[-S_{ab}(t_b)]\}, \end{aligned} \quad (\text{A1})$$

$$\begin{aligned} \mathcal{M}_e^L = & -\frac{8}{3}C_F f_B \pi M_B^4 \int_0^1 dx_2 dx_3 \int_0^\infty b_2 b_3 db_2 db_3 \phi_2(x_2) \phi_3(x_3) \exp(-\frac{b_2^2 \omega_B^2}{2}) \times \\ & \{[1 - x_1 - x_3 + r_2(1 - x_2)] \alpha_s(t_c) h_e(\beta_c, \alpha_e, b_3, b_2) \exp[-S_{cd}(t_c)] - \\ & [1 - x_1 - x_2 + x_3 - r_2(1 - x_2)] \alpha_s(t_d) h_e(\beta_d, \alpha_e, b_3, b_2) \exp[-S_{cd}(t_d)]\}, \end{aligned} \quad (\text{A2})$$

$$\begin{aligned} \mathcal{F}_a^L = & -8C_F f_B \pi M_B^4 \int_0^1 dx_2 dx_3 \int_0^\infty b_2 b_3 db_2 db_3 \phi_2(x_2) \phi_3(x_3) \times \\ & \{[1 - x_2] \alpha_s(t_e) h_e(\alpha_a, \beta_e, b_2, b_3) \exp[-S_{ef}(t_e)] S_t(x_3) - \\ & [1 - x_3] \alpha_s(t_f) h_e(\alpha_a, \beta_f, b_3, b_2) \exp[-S_{ef}(t_f)] S_t(x_2)\}, \end{aligned} \quad (\text{A3})$$



$$\begin{aligned}\mathcal{M}_a^L &= \frac{8}{3}C_F f_B \pi M_B^4 \int_0^1 dx_2 dx_3 \int_0^\infty b_1 b_2 db_1 db_2 \phi_2(x_2) \phi_3(x_3) \exp(-\frac{b_1^2 \omega_B^2}{2}) \times \\ &\quad \{[x_1 + x_3 - 1 - r_c] \alpha_s(t_g) h_e(\beta_g, \alpha_a, b_1, b_2) \exp[-S_{gh}(t_g)] \\ &\quad - [r_b - x_2] \alpha_s(t_h) h_e(\beta_h, \alpha_a, b_1, b_2) \exp[-S_{gh}(t_h)]\},\end{aligned}\quad (\text{A4})$$

$$\begin{aligned}\mathcal{F}_e^N &= -2\sqrt{\frac{2}{3}}C_F f_B f_3 r_3 \pi M_B^4 \int_0^1 dx_2 \int_0^\infty b_1 b_2 db_1 db_2 \phi_2(x_2) \exp(-\frac{b_1^2 \omega_B^2}{2}) \times \\ &\quad \{[2 - r_b + r_2(4r_b - x_2 - 1)] \alpha_s(t_a) h_e(\alpha_e, \beta_a, b_1, b_2) S_t(x_2) \exp[-S_{ab}(t_a)] \\ &\quad - r_2 \alpha_s(t_b) h_e(\alpha_e, \beta_b, b_2, b_1) S_t(x_1) \exp[-S_{ab}(t_b)]\},\end{aligned}\quad (\text{A5})$$

$$\begin{aligned}\mathcal{F}_e^T &= 2\sqrt{\frac{2}{3}}C_F f_B f_3 r_3 \pi M_B^4 \int_0^1 dx_2 \int_0^\infty b_1 b_2 db_1 db_2 \phi_2(x_2) \exp(-\frac{b_1^2 \omega_B^2}{2}) \times \\ &\quad \{[2 - r_b - r_2(1 - x_2)] \alpha_s(t_a) h_e(\alpha_e, \beta_a, b_1, b_2) S_t(x_2) \exp[-S_{ab}(t_a)] \\ &\quad - r_2 \alpha_s(t_b) h_e(\alpha_e, \beta_b, b_2, b_1) S_t(x_1) \exp[-S_{ab}(t_b)]\},\end{aligned}\quad (\text{A6})$$

$$\begin{aligned}\mathcal{M}_e^N &= -\mathcal{M}_e^T = \frac{8}{3}C_F f_B \pi M_B^4 r_3 \int_0^1 dx_2 dx_3 \int_0^\infty b_2 b_3 db_2 db_3 \phi_2(x_2) \phi_3(x_3) \exp(-\frac{b_2^2 \omega_B^2}{2}) \\ &\quad \times \{[x_1 + x_3 - 1] \alpha_s(t_c) h_e(\beta_c, \alpha_e, b_3, b_2) \exp[-S_{cd}(t_c)] - \\ &\quad [x_1 - x_3] \alpha_s(t_d) h_e(\beta_d, \alpha_e, b_3, b_2) \exp[-S_{cd}(t_d)]\},\end{aligned}\quad (\text{A7})$$

$$\begin{aligned}\mathcal{F}_a^N &= -8C_F f_B \pi M_B^4 r_2 r_3 \int_0^1 dx_2 dx_3 \int_0^\infty b_2 b_3 db_2 db_3 \phi_2(x_2) \phi_3(x_3) \times \\ &\quad \{[2 - x_2] \alpha_s(t_e) h_e(\alpha_a, \beta_e, b_2, b_3) \exp[-S_{ef}(t_e)] S_t(x_3) - \\ &\quad [2 - x_3] \alpha_s(t_f) h_e(\alpha_a, \beta_f, b_3, b_2) \exp[-S_{ef}(t_f)] S_t(x_2)\},\end{aligned}\quad (\text{A8})$$

$$\begin{aligned}\mathcal{F}_a^T &= -8C_F f_B \pi M_B^4 r_2 r_3 \int_0^1 dx_2 dx_3 \int_0^\infty b_2 b_3 db_2 db_3 \phi_2(x_2) \phi_3(x_3) \times \\ &\quad \{x_2 \alpha_s(t_e) h_e(\alpha_a, \beta_e, b_2, b_3) \exp[-S_{ef}(t_e)] S_t(x_3) + \\ &\quad x_3 \alpha_s(t_f) h_e(\alpha_a, \beta_f, b_3, b_2) \exp[-S_{ef}(t_f)] S_t(x_2)\},\end{aligned}\quad (\text{A9})$$

$$\begin{aligned}\mathcal{M}_a^N &= \frac{8}{3}C_F f_B \pi M_B^4 \int_0^1 dx_2 dx_3 \int_0^\infty b_1 b_2 db_1 db_2 \phi_2(x_2) \phi_3(x_3) \exp(-\frac{b_1^2 \omega_B^2}{2}) \times \\ &\quad \{[r_2^2(x_2 - 1) + r_3^2(x_3 - 1)] \alpha_s(t_g) h_e(\beta_g, \alpha_a, b_1, b_2) \exp[-S_{gh}(t_g)] \\ &\quad - [r_2^2 x_2 + r_3^2 x_3 - 2r_2 r_3 r_b] \alpha_s(t_h) h_e(\beta_h, \alpha_a, b_1, b_2) \exp[-S_{gh}(t_h)]\},\end{aligned}\quad (\text{A10})$$

$$\begin{aligned}\mathcal{M}_a^T &= \frac{8}{3}C_F f_B \pi M_B^4 \int_0^1 dx_2 dx_3 \int_0^\infty b_1 b_2 db_1 db_2 \phi_2(x_2) \phi_3(x_3) \exp(-\frac{b_1^2 \omega_B^2}{2}) \times \\ &\quad \{[r_2^2(x_2 - 1) - r_3^2(x_3 - 1)] \alpha_s(t_g) h_e(\beta_g, \alpha_a, b_1, b_2) \exp[-S_{gh}(t_g)] \\ &\quad - [r_2^2 x_2 - r_3^2 x_3] \alpha_s(t_h) h_e(\beta_h, \alpha_a, b_1, b_2) \exp[-S_{gh}(t_h)]\}.\end{aligned}\quad (\text{A11})$$

For the CKM suppressed  $B_c \rightarrow D_{(s)}^{*+} D^{*0}$  decays, the decay amplitudes for different polarizations are

$$\begin{aligned} \mathcal{F}_{e2}^L = & -2\sqrt{\frac{2}{3}}C_F f_B f_3 \pi M_B^4 \int_0^1 dx_2 \int_0^\infty b_1 b_2 db_1 db_2 \phi_2(x_2) \exp(-\frac{b_1^2 \omega_B^2}{2}) \times \\ & \{[-(r_2 - 2)r_b + 2r_2 x_2 - x_2] \alpha_s(t_a) h_e(\alpha_e, \beta_a, b_1, b_2) S_t(x_2) \exp[-S_{ab}(t_a)] \\ & + r_2^2 \alpha_s(t_b) h_e(\alpha_e, \beta_b, b_2, b_1) S_t(x_1) \exp[-S_{ab}(t_b)]\}, \end{aligned} \quad (\text{A12})$$

$$\begin{aligned} \mathcal{F}_{e2}^N = & -2\sqrt{\frac{2}{3}}C_F f_B f_3 r_3 \pi M_B^4 \int_0^1 dx_2 \int_0^\infty b_1 b_2 db_1 db_2 \phi_2(x_2) \exp(-\frac{b_1^2 \omega_B^2}{2}) \times \\ & \{[2 - r_b + r_2(4r_b - x_2 - 1)] \alpha_s(t_a) h_e(\alpha_e, \beta_a, b_1, b_2) S_t(x_2) \exp[-S_{ab}(t_a)] \\ & - r_2 \alpha_s(t_b) h_e(\alpha_e, \beta_b, b_2, b_1) S_t(x_1) \exp[-S_{ab}(t_b)]\}, \end{aligned} \quad (\text{A13})$$

$$\begin{aligned} \mathcal{F}_{e2}^T = & 2\sqrt{\frac{2}{3}}C_F f_B f_3 r_3 \pi M_B^4 \int_0^1 dx_2 \int_0^\infty b_1 b_2 db_1 db_2 \phi_2(x_2) \exp(-\frac{b_1^2 \omega_B^2}{2}) \times \\ & \{[2 - r_b - r_2(1 - x_2)] \alpha_s(t_a) h_e(\alpha_e, \beta_a, b_1, b_2) S_t(x_2) \exp[-S_{ab}(t_a)] \\ & - r_2 \alpha_s(t_b) h_e(\alpha_e, \beta_b, b_2, b_1) S_t(x_1) \exp[-S_{ab}(t_b)]\}, \end{aligned} \quad (\text{A14})$$

$$\begin{aligned} \mathcal{M}_{e2}^L = & \frac{8}{3}C_F f_B \pi M_B^4 \int_0^1 dx_2 dx_3 \int_0^\infty b_2 b_3 db_2 db_3 \phi_2(x_2) \phi_3(x_3) \exp(-\frac{b_1^2 \omega_B^2}{2}) \times \\ & \{[2 - x_1 - x_2 - x_3 - r_2(1 - x_2)] \alpha_s(t_c) h_e(\beta_c, \alpha_e, b_3, b_2) \exp[-S_{cd}(t_c)] - \\ & [x_3 - x_1 + r_2(1 - x_2)] \alpha_s(t_d) h_e(\beta_d, \alpha_e, b_3, b_2) \exp[-S_{cd}(t_d)]\}, \end{aligned} \quad (\text{A15})$$

$$\begin{aligned} \mathcal{M}_{e2}^N = & -\mathcal{M}_{e2}^T = \frac{8}{3}C_F f_B \pi M_B^4 \int_0^1 dx_2 dx_3 \int_0^\infty b_2 b_3 db_2 db_3 \phi_2(x_2) \phi_3(x_3) \exp(-\frac{b_1^2 \omega_B^2}{2}) \\ & \times \{[r_3(x_1 - x_3)] \alpha_s(t_c) h_e(\beta_c, \alpha_e, b_3, b_2) \exp[-S_{cd}(t_c)] + \\ & [2r_c - r_3(1 - x_1 - x_3)] \alpha_s(t_d) h_e(\beta_d, \alpha_e, b_3, b_2) \exp[-S_{cd}(t_d)]\}. \end{aligned} \quad (\text{A16})$$

## Appendix B: Scales and related functions in hard kernel

We show here the functions  $h_e$ , coming from the Fourier transform of hard kernel,

$$\begin{aligned} h_e(\alpha, \beta, b_1, b_2) &= h_1(\alpha, b_1) \times h_2(\beta, b_1, b_2), \\ h_1(\alpha, b_1) &= \begin{cases} K_0(\sqrt{\alpha} b_1), & \alpha > 0 \\ K_0(i\sqrt{-\alpha} b_1), & \alpha < 0 \end{cases} \\ h_2(\beta, b_1, b_2) &= \begin{cases} \theta(b_1 - b_2) I_0(\sqrt{\beta} b_2) K_0(\sqrt{\beta} b_1) + (b_1 \leftrightarrow b_2), & \beta > 0 \\ \theta(b_1 - b_2) J_0(\sqrt{-\beta} b_2) K_0(i\sqrt{-\beta} b_1) + (b_1 \leftrightarrow b_2), & \beta < 0 \end{cases} \end{aligned} \quad (\text{B1})$$

where  $J_0$  is the Bessel function and  $K_0, I_0$  are modified Bessel function with  $K_0(ix) = \frac{\pi}{2}(-N_0(x) + iJ_0(x))$ . The hard scale  $t$  is chosen as the maximum virtuality of the internal momentum transition in the hard amplitudes, including  $1/b_i (i = 1, 2, 3)$ :

$$\begin{aligned} t_a &= \max(\sqrt{|\alpha_e|}, \sqrt{|\beta_a|}, 1/b_1, 1/b_2), & t_b &= \max(\sqrt{|\alpha_e|}, \sqrt{|\beta_b|}, 1/b_1, 1/b_2), \\ t_c &= \max(\sqrt{|\alpha_e|}, \sqrt{|\beta_c|}, 1/b_2, 1/b_3), & t_d &= \max(\sqrt{|\alpha_e|}, \sqrt{|\beta_d|}, 1/b_2, 1/b_3), \\ t_e &= \max(\sqrt{|\alpha_a|}, \sqrt{|\beta_e|}, 1/b_2, 1/b_3), & t_f &= \max(\sqrt{|\alpha_a|}, \sqrt{|\beta_f|}, 1/b_2, 1/b_3), \\ t_g &= \max(\sqrt{|\alpha_a|}, \sqrt{|\beta_g|}, 1/b_1, 1/b_2), & t_h &= \max(\sqrt{|\alpha_a|}, \sqrt{|\beta_h|}, 1/b_1, 1/b_2), \end{aligned} \quad (\text{B2})$$

where

$$\begin{aligned} \alpha_e &= (1 - x_2)(x_1 - r_2^2)(1 - r_3^2)M_B^2, & \alpha_a &= -(1 + (r_3^2 - 1)x_2)(1 + (r_2^2 - 1)x_3)M_B^2, \\ \beta_a &= [r_b^2 + (r_2^2 - 1)(x_2 + r_3^2(1 - x_2))]M_B^2, & \beta_b &= (1 - r_3^2)(x_1 - r_2^2)M_B^2, \\ \beta_c &= [r_c^2 - (1 - x_2(1 - r_3^2))(1 - x_1 - x_3(1 - r_2^2))]M_B^2, \\ \beta_d &= (1 - x_2)(1 - r_3^2)[x_1 - x_3 - r_2^2(1 - x_3)]M_B^2, \\ \beta_e &= -[1 + (r_3^2 - 1)x_2]M_B^2, & \beta_f &= -[1 + (r_2^2 - 1)x_3]M_B^2, \\ \beta_g &= [r_c^2 + (1 - x_2(1 - r_3^2))(x_1 + x_3 - 1 - r_2^2x_3)]M_B^2, \\ \beta_h &= [r_b^2 - x_2(r_3^2 - 1)(x_1 - x_3(1 - r_2^2))]M_B^2. \end{aligned} \quad (\text{B3})$$

The Sudakov factors used in the text are defined by

$$\begin{aligned} S_{ab}(t) &= s\left(\frac{M_B}{\sqrt{2}}x_1, b_1\right) + s\left(\frac{M_B}{\sqrt{2}}x_2, b_2\right) + \frac{5}{3} \int_{1/b_1}^t \frac{d\mu}{\mu} \gamma_q(\mu) + 2 \int_{1/b_2}^t \frac{d\mu}{\mu} \gamma_q(\mu), \\ S_{cd}(t) &= s\left(\frac{M_B}{\sqrt{2}}x_1, b_2\right) + s\left(\frac{M_B}{\sqrt{2}}x_2, b_2\right) + s\left(\frac{M_B}{\sqrt{2}}x_3, b_3\right) \\ &\quad + \frac{11}{3} \int_{1/b_2}^t \frac{d\mu}{\mu} \gamma_q(\mu) + 2 \int_{1/b_3}^t \frac{d\mu}{\mu} \gamma_q(\mu), \\ S_{ef}(t) &= s\left(\frac{M_B}{\sqrt{2}}x_2, b_2\right) + s\left(\frac{M_B}{\sqrt{2}}x_3, b_3\right) + 2 \int_{1/b_2}^t \frac{d\mu}{\mu} \gamma_q(\mu) + 2 \int_{1/b_3}^t \frac{d\mu}{\mu} \gamma_q(\mu), \\ S_{gh}(t) &= s\left(\frac{M_B}{\sqrt{2}}x_1, b_1\right) + s\left(\frac{M_B}{\sqrt{2}}x_2, b_2\right) + s\left(\frac{M_B}{\sqrt{2}}x_3, b_2\right), \\ &\quad + \frac{5}{3} \int_{1/b_1}^t \frac{d\mu}{\mu} \gamma_q(\mu) + 4 \int_{1/b_2}^t \frac{d\mu}{\mu} \gamma_q(\mu), \end{aligned} \quad (\text{B4})$$

where the functions  $s(Q, b)$  are defined in Appendix A of [24].  $\gamma_q = -\alpha_s/\pi$  is the anomalous dimension of the quark.

## Appendix C: Meson Wave functions

In the nonrelativistic limit, the  $B_c$  meson wave function can be written as [33]

$$\Phi_{B_c}(x) = \frac{if_B}{4N_c}[(P + M_{B_c})\gamma_5\delta(x - r_c)]\exp(-\frac{b^2\omega_B^2}{2}), \quad (C1)$$

in which the last exponent term represents the  $k_T$  distribution. Here, we only consider the dominant Lorentz structure and neglect another contribution in our calculation [34].

In the heavy quark limit, the two-particle light-cone distribution amplitudes of  $D_{(s)}/D_{(s)}^*$  meson are defined as [35]

$$\begin{aligned} \langle D_{(s)}(P_2)|q_\alpha(z)\bar{c}_\beta(0)|0\rangle &= \frac{i}{\sqrt{2N_c}}\int_0^1 dx e^{ixP_2\cdot z}[\gamma_5(P_2 + m_{D_{(s)}})\phi_{D_{(s)}}(x, b)]_{\alpha\beta}, \\ \langle D_{(s)}^*(P_2)|q_\alpha(z)\bar{c}_\beta(0)|0\rangle &= -\frac{1}{\sqrt{2N_c}}\int_0^1 dx e^{ixP_2\cdot z}[\not{e}_L(P_2 + m_{D_{(s)}^*})\phi_{D_{(s)}^*}^L(x, b) \\ &\quad + \not{e}_T(P_2 + m_{D_{(s)}^*})\phi_{D_{(s)}^*}^T(x, b)]_{\alpha\beta}, \end{aligned} \quad (C2)$$

with the normalization conditions:

$$\int_0^1 dx \phi_{D_{(s)}}(x, 0) = \frac{f_{D_{(s)}}}{2\sqrt{2N_c}}, \quad \int_0^1 dx \phi_{D_{(s)}^*}^L(x, 0) = \int_0^1 dx \phi_{D_{(s)}^*}^T(x, 0) = \frac{f_{D_{(s)}^*}}{2\sqrt{2N_c}}, \quad (C3)$$

where we have assumed  $f_{D_{(s)}^*} = f_{D_{(s)}^*}^T$ . Note that equations of motion do not relate  $\phi_{D_{(s)}^*}^L$  and  $\phi_{D_{(s)}^*}^T$ . We use the following relations derived from HQET [36] to determine  $f_{D_{(s)}^*}$

$$f_{D_{(s)}^*} = \sqrt{\frac{m_{D_{(s)}}}{m_{D_{(s)}^*}}} f_{D_{(s)}}. \quad (C4)$$

The distribution amplitude  $\phi_{D_{(s)}^*}^{(L,T)}$  is taken as [18]

$$\phi_{D_{(s)}^*}^{(L,T)} = \frac{3}{\sqrt{2N_c}} f_{D_{(s)}^*} x(1-x)[1 + a_{D_{(s)}^*}(1-2x)] \exp(-\frac{b^2\omega_{D_{(s)}}^2}{2}). \quad (C5)$$

We use  $a_D = 0.5 \pm 0.1, \omega_D = 0.1\text{GeV}$  for  $D/D^*$  meson and  $a_{D_s} = 0.4 \pm 0.1, \omega_{D_s} = 0.2\text{GeV}$  for  $D_s/D_s^*$  meson, which are determined in Ref. [20] by fitting.

- 
- [1] N. Brambilla et al., (Quarkonium Working Group), CERN-2005-005, hep-ph/0412158.
  - [2] M. Masetti, Phys. Lett. B **286**, 160 (1992).

- [3] R. Fleischer and D. Wyler, Phys. Rev. D **62**, 057503 (2000); R. Fleischer, Lect. Notes Phys. **647**, 42 (2004).
- [4] V.V. Kiselev, J. Phys. G **30**, 1445 (2004); V.V. Kiselev, A. E. Kovalsky, and A.K. Likhoded, Nucl. Phys. B **585**, 353 (2000); V.V. Kiselev, arXiv:hep-ph/ 0211021.
- [5] M.A. Ivanov, J.G. Körner and O.N. Pakhomova, Phys. Lett. B **555**, 189 (2003).
- [6] A. K. Giri, R. Mohanta and M. P. Khanna, Phys. Rev. D **65**, 034016 (2001).
- [7] M.A. Ivanov, J.G. Körner and P. Santorelli, Phys. Rev. D **73**, 054024 (2006).
- [8] Jia-Fu Liu and Kuang-Ta Chao, Phys. Rev. D **56**, 4133 (1997).
- [9] I. P. Gouz, V. V. Kiselev, A. K. Likhoded, V. I. Romanovsky, and O. P. Yushchenko, Phys. Atom. Nucl. **67**, 1559 (2004); Yad. Fiz. **67**, 1581 (2004).
- [10] P. Colangelo and F. De Fazio, Phys. Rev. D **61**, 034012 (2000).
- [11] A. Abd El-Hady, J.H. Munoz, and J. P. Vary, Phys. Rev. D **62**, 014019 (2000).
- [12] C.H. Chang and Y.Q. Chen, Phys. Rev. D **49**, 3399 (1994).
- [13] Hai-Yang Cheng, Chun-Khiang Chua, Phys. Rev. D **80**, 114008 (2009).
- [14] H.-n. Li, and H.L.Yu, Phys. Rev. Lett. **74**, 4388 (1995); H.-n. Li, Phys. Lett. B **348**, 597 (1995).
- [15] Y. Y. Keum, H. n. Li and A. I. Sanda, Phys. Lett. B **504**, 6 (2001).
- [16] Cai-Dian Lü, K. Ukai and M.-Z. Yang, Phys. Rev. D **63**, 074009 (2001); Cai-Dian Lü and M.Z. Yang, Eur. Phys. J. C **23**, 275 (2002).
- [17] C.W.Bauer, S. Fleming, D. Pirjol and I. W. Stewart, Phys. Rev. D **63**, 114020 (2001); C.W.Bauer, D. Pirjol and I. W. Stewart, Phys. Rev. Lett. **87**, 201806 (2001); Phys. Rev. D **65**, 054022 (2002).
- [18] Run-Hui Li, Cai-Dian Lü, and Hao Zou, Phys. Rev. D **78**, 014018 (2008); Hao Zou, Run-Hui Li, Xiao-Xia Wang, and Cai-Dian Lü, J. Phys. G: Nucl. Part. Phys. **37**, 015002 (2010).
- [19] Ying Li, Cai-Dian Lü and Cong-Feng Qiao, Phys. Rev. D **73**, 094006 (2006); Ying Li and Cai-Dian Lü, J. Phys. G **29**, 2115 (2003);
- [20] Run-Hui Li, Cai-Dian Lü, A.I. Sanda and Xiao-Xia Wang, Phys. Rev. D **81**, 034006 (2010).
- [21] Ying Li, Cai-Dian Lü and Zhen-Jun Xiao, J. Phys. G **31**, 273 (2005).
- [22] J. C. Collins and D. E. Soper, Nucl. Phys. B **193**, 381 (1981); J. Botts and G. Sterman, Nucl. Phys. B **325**, 62 (1989).
- [23] B. Melic, B. Nizic, and K. Passek, Phys. Rev. D **60**, 074004 (1999).

- [24] Jian-Feng Cheng, Dong-Sheng Du, and Cai-Dian Lü, Eur. Phys. J. C. **45**, 711 (2006).
- [25] Cai-Dian Lü, Phys. Rev. D **68**, 097502 (2003); Yong-Yeon Keum, et al, Phys. Rev. D **69** , 094018 (2004).
- [26] Particle Data Group, J. Phys. G: Nucl.Part. Phys. **37**, 075021 (2010).
- [27] W.Wang,Y.L.Shen and C.D. Lü, Phys. Rev. D **79**, 054012 (2009).
- [28] R. Dhir, N. Sharma, and R. C. Verma, J. Phys. G **35**, 085002 (2008); R.C. Verma and A. Sharma, Phys. Rev. D **65**, 114007 (2002); R. Dhir and R.C. Verma, Phys. Rev. D **79**, 034004 (2009).
- [29] Dong-Sheng Du and Z. Wang, Phys. Rev. D **39**, 1342 (1989).
- [30] Ahmed Ali, G. Kramer, Cai-Dian Lü, Phys. Rev. D **58**, 094009 (1998).
- [31] Ying Li and Cai-Dian Lü, Phys. Rev. D **73**, 014024 (2006).
- [32] Zhou Rui, Zhi-Tian Zou and Cai-Dian Lü, arXiv: 1112.1257 [hep-ph].
- [33] Xin Liu, Zhen-Jun Xiao, and Cai-Dian Lü, Phys. Rev. D **81**, 014022 (2010).
- [34] Cai-Dian Lü, M.-Z. Yang, Eur. Phys. J. C **28**, 515 (2003).
- [35] T. Kurimoto, H. n. Li and A. I. Sanda, Phys. Rev. D **67**, 054028 (2003).
- [36] A. V. Manohar and M. B. Wise, Camb. Monogr. Part. Phys. Nucl. Phys. Cosmol. **10**, 1 (2000).